ACHIEVING ACCOMPANYING BEAMPATTERN PEAK FOR HIGH-SPEED USERS VIA FREQUENCY DIVERSE ARRAY

Jingran Lin, Qiang Li, and Dongmei Zhao

School of Information and Communication Engineering
University of Electronic Science and Technology of China, Chengdu China, 611731

ABSTRACT

In this paper, we consider how to maintain the communication quality for high-speed users in array transmission. Due to high user speed, the array transmission angle changes quickly. As a consequence, the phase shifters (beamformers) of traditional phase arrays need to be updated frequently to aim at the user, thus yielding high implementation cost. To alleviate this, we propose a novel frequency diverse array (FDA) approach, which intentionally introduces some frequency offsets across the array antennas to activate an *angle-range-time* dependent beampattern; i.e., the FDA beampattern peak automatically moves in space. This motivates us to carefully design FDA parameters such that the beampattern peak accompanies the quickly-moving users. To this end, we maximize the average beampattern gain along some given user trace by optimizing the frequency offsets. The block successive upper-bound minimization (BSUM) method is applied to obtain a stationary solution to this non-convex problem. Compared with phase array beamforming, the FDA approach maintains service quality for high-speed users by updating frequency offsets less frequently, thus reducing the implementation cost remarkably.

Index Terms— Frequency diverse array (FDA), high-speed user, accompanying beampattern peak, frequency offset, block successive upper-bound maximization (BSUM).

1. INTRODUCTION

With the rapid development of bullet train and high-speed rail technologies, a travelling speed as high as 350km/h is already available at present [1]. This has greatly facilitated people's life. Meanwhile, a challenging problem arises — how to maintain the communication quality for high-speed users?

Array processing techniques have been widely utilized in modern communication systems to enhance service quality. For instance, in traditional phase diverse array (PDA), phase shifters (beamformers) can be used to tune the array to aim at the user to improve signal integrity [2, 3]. However, due to the fixed phase lags among antennas, the angle-dependent PDA beampattern does not vary with time, as shown in Fig. 1(a). In high-speed user scenarios, the array transmission angle changes quickly. As a consequence, the phase shifters must be frequently updated to maintain service quality, thus rendering high implementation cost for PDA approaches.

To tackle this, we propose a novel frequency diverse array (FDA) approach in this paper. As shown in Fig. 1(b), FDA introduces small frequency offsets across the array antennas, and hence the phase lags among different antennas accumulate as the radio wave propagates in space; finally, an *angle-range-time-dependent* beampattern will be generated [4, 5]. Different from the static PDA beampattern, the "S-shape" FDA beampattern is time-varying, and the beampattern peak moves in space automatically during signal propagation. The beampattern peak trace of FDA is related to the instantaneous phase lags among antennas, which is essentially determined by the frequency offsets. This motivates us to judiciously design the FDA frequency offsets such that the resultant peak trace of FDA beampattern coincides with the user trace within a specific time period; namely, let the beampattern peak accompany the quickly-moving users. Compared with the traditional PDA approaches, the proposed method maintains service quality for high-speed users by updating frequency offsets less frequently, thus reducing the implementation cost remarkably.

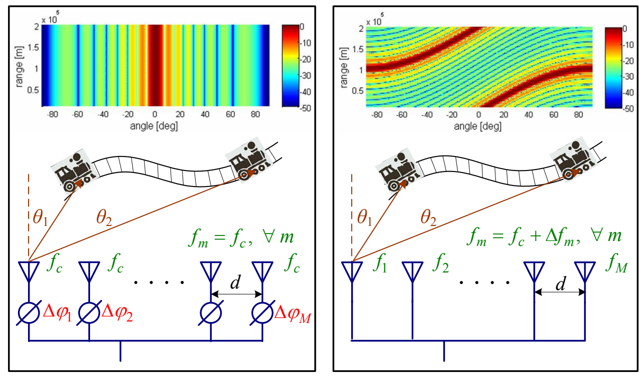

(a) Phase diverse array (b) Frequency diverse array

Fig. 1. Phase diverse array and frequency diverse array

To the best of our knowledge, so far no related research has been reported. Current studies on FDA mainly consider its application in radar and navigation systems [6–10]. In addition, there are several studies addressing the FDA-based secure communication problems [11–14]. Departing from these works, we study an FDA beampattern peak trace fitting problem in this paper. To this end, we maximize the average beampattern gain along some given user trace by optimizing the frequency offsets. This is a difficult non-convex problem. Hence, we are driven to pursue some suboptimal solution with manageable complexity. Specifically, we apply the block successive upper-bound minimization (BSUM) method [15] to iteratively find a solution with stationary convergence guarantee. Each step of BSUM has a simple closed-form solution, thus giving the algorithm very low complexity.

2. DATA MODEL AND PROBLEM STATEMENT

As shown in Fig. 1(b), we consider a uniform linear transmit array consisting of M antennas, which forwards information to a single-

This work was supported by the National Natural Science Foundation of China [61671120, 61531009, 61471103] and the Fundamental Research Funds for the Central Universities [ZYGX2016J007, ZYGX2016J011].

antenna high-speed user. As opposed to the conventional PDA, FDA employs small frequency offsets across the array antennas. Specifically, the radiation frequency of the mth antenna is $f_m = f_c + \Delta f_m$ for $m = 1, 2, \dots, M$, with f_c and Δf_m being the carrier frequency and the frequency offsets, respectively. We assume $|\Delta f_m| \leq \Delta F$ and $\Delta F \ll f_c$ here. Let d denote the uniform antenna spacing of the transmit array, which is set as $d = c/[2(f_c + \Delta F)] \simeq c/(2f_c)$ to avoid aliasing effects with c being the speed of light.

Without loss of generality, we set the first antenna as the origin of the $(range, angle)$ coordinate system. For the user at (r, θ), the directional channel[1] with the mth antenna is defined as [6, 11, 12]

$$h_m(f_m, r, \theta, t) = a(r) e^{-j2\pi(f_c+\Delta f_m)\left[t - \frac{r-(m-1)d\sin\theta}{c}\right]}, \quad (1)$$

where $a(r)$ is the signal attenuation factor at the range of r. Then, we compute the FDA beampattern gain at (r, θ) as

$$\begin{aligned} |\mathrm{B}(\mathbf{f}, r, \theta, t)| &= \left|\sum_{m=1}^{M} h_m(f_m, r, \theta, t)\right| \\ &= a(r)\left|\sum_{m=1}^{M} e^{-j2\pi\left\{f_c\frac{(m-1)d\sin\theta}{c} + \Delta f_m\left[t - \frac{r-(m-1)d\sin\theta}{c}\right]\right\}}\right| \\ &= a(r)\left|\sum_{m=1}^{M} e^{j[\Phi_{0,m}(\theta) + \Phi_{1,m}(\Delta f_m, r, \theta, t)]}\right| \quad (2) \end{aligned}$$

where $\mathbf{f} = [f_1, f_2, \dots, f_M]^T$; $\Phi_{0,m}(\theta) = -2\pi f_c \frac{(m-1)d\sin\theta}{c}$, and $\Phi_{1,m}(\Delta f_m, r, \theta, t) = -2\pi\Delta f_m[t - \frac{r-(m-1)d\sin\theta}{c}]$, $\forall m$.

In the case of $\Delta f_m = 0$, we have $\Phi_{1,m}(\Delta f_m, r, \theta, t) = 0$ for $m = 1, 2, \dots, M$, and FDA reduces to the conventional PDA. Thus, the beampattern gain depends on θ only and does not vary with time. As a contrast, nonzero $\Phi_{1,m}(\Delta f_m, r, \theta, t)$ will be activated in FDA as $\Delta f_m \neq 0$ for $m = 1, 2, \dots, M$, thus yielding distinct accumulating phase lags among array antennas. Consequently, the beampattern of FDA depends on the frequency offsets $\{\Delta f_m\}_{m=1}^{M}$, the range r, the angle θ, and the time t. This explains why the FDA beampattern peak can move in space even with fixed frequency offsets.

Although the FDA beampattern peak moves automatically, there is no guarantee that the peak trace will coincide with the user trace using some randomly chosen frequency offsets. Define $r(t)$ and $\theta(t)$ as the user traces in range and angle dimensions. To let the beampattern peak accompany the user within the time period $[T_1, T_2]$, we optimize the frequency offsets to maximize the average beampattern gain along the user trace $(r(t), \theta(t)), \forall\, t \in [T_1, T_2]$, i.e.,

$$\begin{aligned} \max_{\mathbf{f}} \quad & \frac{1}{T_2 - T_1}\int_{T_1}^{T_2} |\mathrm{B}(\mathbf{f}, r(t), \theta(t), t)|^2\, dt \quad (\mathrm{P1}) \\ \text{s.t.} \quad & f_c - \Delta F \leq f_m \leq f_c + \Delta F,\ \forall\, m. \quad (3) \end{aligned}$$

In brief, our target is to appropriately select the frequency offsets within the range $[-\Delta F, \Delta F]$, such that the FDA beampattern peak trace maximally fits the user trace. As a consequence, in time period $[T_1, T_2]$, high service quality can be maintained for quickly-moving users without changing the frequency offsets.

Remark 1. *For long user trace or complicated user trace, we can split it into multiple segments, and design different frequency offsets for distinct segments. Hence, high service quality can be maintained by updating the frequency offsets with low frequency. Due to space limitation, we address the trace fitting problem in only one segment here, and the multi-segment trace fitting problem will be considered in the journal version.*

[1] We have ignored the very few multi-path components (MPCs) here. This is acceptable since in many high-frequency (e.g., millimeter-wave (mmWave) bands) transmission systems, the MPCs were found to be attenuated by 20dB compared to the direct component [16].

3. ALGORITHM FOR FREQUENCY OFFSETS DESIGN

Obviously, (P1) is a difficult non-convex problem. We are thus driven to pursue some suboptimal solution with manageable complexity.

To avoid directly handling the integral, we first approximate the objective by the average of K samples of beampattern gain, i.e.,

$$\begin{aligned} &\frac{1}{T_2 - T_1}\int_{T_1}^{T_2} |\mathrm{B}(\mathbf{f}, r(t), \theta(t), t)|^2\, dt \\ \simeq &\frac{1}{K}\sum_{k=1}^{K} |\mathrm{B}(\mathbf{f}, r(t_k), \theta(t_k), t_k)|^2, \quad (4) \end{aligned}$$

where $T_1 \leq t_k \leq T_2$ for $k = 1, 2, \dots, K$.

For notational simplicity, we use r_k and θ_k to denote $r(t_k)$ and $\theta(t_k)$, and define $\tau_{m,k} \triangleq t_k - \frac{r_k-(m-1)d\sin\theta_k}{c}$, $\forall\, m, k$. Then, we have

$$\begin{aligned} |\mathrm{B}(\mathbf{f}, r_k, \theta_k, t_k)|^2 &= a^2(r_k)\left|\sum_{m=1}^{M} e^{-j2\pi f_m \tau_{m,k}}\right|^2 \\ &= a^2(r_k)\left\{M + \sum_{m=1}^{M}\sum_{\substack{n=1 \\ n\neq m}}^{M} \cos\left[2\pi(f_m\tau_{m,k} - f_n\tau_{n,k})\right]\right\}, \quad (5) \end{aligned}$$

and (P1) can be handled by solving the following problem

$$\begin{aligned} \max_{\mathbf{f}} \quad & \sum_{k=1}^{K} a^2(r_k)\sum_{m=1}^{M}\sum_{\substack{n=1 \\ n\neq m}}^{M} \cos\left[2\pi(f_m\tau_{m,k} - f_n\tau_{n,k})\right] \quad (\mathrm{P2}) \\ \text{s.t.} \quad & f_c - \Delta F \leq f_m \leq f_c + \Delta F,\ \forall\, m. \end{aligned}$$

To solve (P2), we resort to the block successive upper-bound minimization (BSUM) method [15], which is a very general framework to handle a general non-convex non-smooth problem with multiple block variables. Since our algorithm relies heavily on BSUM, let us first give a brief review of the BSUM method.

3.1. A Brief Review of the BSUM Method

Consider the following minimization problem,

$$\begin{aligned} \min_{\mathbf{x}} \ & y(x_1, x_2, ..., x_I) \\ \text{s.t.} \ & x_i \in \mathcal{X}_i,\ i = 1, 2, ..., I, \end{aligned}$$

where $\mathbf{x} = [x_1, x_2, ..., x_I]^T \in \mathbb{R}^{I\times 1}$; $\mathcal{X}_i \subseteq \mathbb{R}$ is a closed convex set; $y(\cdot) : \prod_{i=1}^{I}\mathcal{X}_i = \mathcal{X} \to \mathbb{R}$ is a continuous function. One popular approach for the above problem is the block coordinate descent (BCD) method [17]. At each iteration of BCD, the function is minimized with respect to a single block while the rest blocks are held fixed. More specifically, in the sth iteration, we update $\mathbf{x}$ as follows

$$\begin{cases} x_i^s = \operatorname{argmin}_{x_i \in \mathcal{X}_i}\ y_i(x_i; \mathbf{x}_{-i}^{s-1}) \\ x_l^s = x_l^{s-1},\ \forall\, l \neq i, \end{cases}$$

where $\mathbf{x}_{-i}^{s-1} \triangleq [x_1^{s-1}, ..., x_{i-1}^{s-1}, x_{i+1}^{s-1}, ..., x_I^{s-1}]^T \in \mathbb{R}^{(I-1)\times 1}$ is the remaining subvector of $\mathbf{x}^{s-1}$ after removing x_i^{s-1}, and $y_i(x_i; \mathbf{x}_{-i}^{s-1}) \triangleq y(x_1^{s-1}, ..., x_{i-1}^{s-1}, x_i, x_{i+1}^{s-1}, ..., x_I^{s-1})$.

However, solving the subproblem may not be easy in the case of non-convex $y_i(x_i; \mathbf{x}_{-i}^{s-1})$. To circumvent this difficulty, the BSUM method proposes to approximate $y_i(x_i;\mathbf{x}_{-i}^{s-1})$ by $u_i(x_i;\mathbf{x}^{s-1}) \triangleq u_i(x_i;x_1^{s-1},x_2^{s-1},...,x_I^{s-1})$, which satisfies

$$\begin{cases} u_i(x_i^{s-1};\mathbf{x}^{s-1}) = y_i(x_i^{s-1};\mathbf{x}_{-i}^{s-1}), \\ u_i'(x_i^{s-1};\mathbf{x}^{s-1}) = y_i'(x_i^{s-1};\mathbf{x}_{-i}^{s-1}), \\ u_i(x_i;\mathbf{x}^{s-1}) \geq y_i(x_i;\mathbf{x}_{-i}^{s-1}), \\ u_i(x_i;\mathbf{x}^{s-1}) \text{ is continuous,} \end{cases} \tag{6}$$

and then updates x_i as

$$\begin{cases} x_i^s = \operatorname{argmin}_{x_i \in \mathcal{X}_i} \ u_i(x_i;\mathbf{x}^{s-1}), \\ x_l^s = x_l^{s-1}, \ \forall\, l \neq i. \end{cases}$$

The convergence of BSUM is summarized below.

Theorem 1 ([15, Theorem 2])**.** *Suppose that: (i) the BSUM assumption* (6) *holds; (ii) the function $u_i(x_i;\mathbf{x}^{s-1})$ is quasi-convex in x_i; (iii) the subproblem in each iteration has a unique solution for any $\mathbf{x}^{s-1} \in \mathcal{X}$; (iv) the function $y(\cdot)$ is regular at every point in the stationary points set. Then, every limit point of the iterates generated by the BSUM algorithm is a stationary point.*

3.2. The BSUM Algorithm for Frequency Offsets Design

Without loss of generality, let us consider the update of f_m in the sth iteration by solving the following problem,

$$\max_{f_m} \ \sum_{k=1}^{K} a^2(r_k) \sum_{\substack{n=1\\n\neq m}}^{M} \cos[2\pi(f_m\tau_{m,k} - f_n^{s-1}\tau_{n,k})] \tag{P3}$$

$$\text{s.t. } f_c - \Delta F \leq f_m \leq f_c + \Delta F. \tag{7}$$

Following BSUM framework, we propose to approximate the non-concave objective of (P3) by some concave quadratic function. For ease of exposition, let us first define the objective of (P3) as

$$y_m(f_m;\mathbf{f}_{-m}^{s-1}) \triangleq \sum_{k=1}^{K} a^2(r_k) \sum_{n=1}^{M} \tilde{y}_{m,n,k}(f_m;f_n^{s-1}) \tag{8}$$

$$\tilde{y}_{m,n,k}(f_m;f_n^{s-1}) \triangleq \begin{cases} \cos[2\pi(f_m\tau_{m,k} - f_n^{s-1}\tau_{n,k})], \ n \neq m, \\ 0, \ \ n = m, \end{cases} \tag{9}$$

and then approximate $y_m(f_m;\mathbf{f}_{-m}^{s-1})$ with some concave quadratic function $u_m(f_m;\mathbf{f}^{s-1})$, i.e.,

$$u_m(f_m;\mathbf{f}^{s-1}) \triangleq \sum_{k=1}^{K} a^2(r_k) \sum_{n=1}^{M} \tilde{u}_{m,n,k}(f_m;f_m^{s-1},f_n^{s-1}), \tag{10}$$

$$\tilde{u}_{m,n,k}(f_m;f_m^{s-1},f_n^{s-1}) \triangleq \begin{cases} \kappa_{m,n,k}(f_m - \zeta_{m,n,k})^2 + \delta_{m,n,k}, \\ \hfill n \neq m, \\ 0, \ \ n = m, \end{cases} \tag{11}$$

where $\kappa_{m,n,k} \in \mathbb{R}_-$, $\zeta_{m,n,k} \in \mathbb{R}$ and $\delta_{m,n,k} \in \mathbb{R}$, $n \neq m$, are parameters needed to be designed; we will elaborate on this shortly.

Therefore, (P3) is replaced by

$$\begin{aligned} \max_{f_m} \ & \sum_{k=1}^{K} a^2(r_k) \sum_{n=1}^{M} \left[\kappa_{m,n,k}(f_m - \zeta_{m,n,k})^2 + \delta_{m,n,k}\right] \\ \text{s.t. } & f_c - \Delta F \leq f_m \leq f_c + \Delta F. \end{aligned}$$

It is easy to show that the optimal solution of the above problem is given by

$$f_m^s = \left[\frac{\sum_{k=1}^{K} a^2(r_k) \sum_{n=1}^{M} \kappa_{m,n,k}\zeta_{m,n,k}}{\sum_{k=1}^{K} a^2(r_k) \sum_{n=1}^{M} \kappa_{m,n,k}}\right]_{f_c-\Delta F}^{f_c+\Delta F}, \tag{12}$$

where $[\,\cdot\,]_{f_c-\Delta F}^{f_c+\Delta F}$ denotes the projection onto $[f_c - \Delta F, \ f_c + \Delta F]$. Algorithm 1 in Table 1 summarizes the procedure to solve (P2). The convergence of Algorithm 1 is established as follows.

Proposition 1. *Every limit point of the iterates generated by Algorithm 1 is a stationary solution of* (P2)*.*

The key step of the proof is to show that the convergence conditions required by BSUM (cf. Theorem 1) are satisfied by Algorithm 1. The details are omitted due to the space limitation.

Next, let us turn back to the design of the BSUM parameters of $\{\kappa_{m,n,k}, \zeta_{m,n,k}, \delta_{m,n,k}\}$ such that the BSUM assumption (6) can be satisfied. Specifically, as shown in Fig. 2, we require that

$$\begin{cases} \tilde{u}_{m,n,k}(f_m^{s-1};f_m^{s-1},f_n^{s-1}) = \tilde{y}_{m,n,k}(f_m^{s-1};f_n^{s-1}) \\ \tilde{u}_{m,n,k}'(f_m^{s-1};f_m^{s-1},f_n^{s-1}) = \tilde{y}_{m,n,k}'(f_m^{s-1};f_n^{s-1}) \\ \tilde{y}_{m,n,k}(\zeta_{m,n};f_n^{s-1}) \geq \tilde{y}_{m,n,k}(f_m^{s-1};f_n^{s-1}) \\ \tilde{y}_{m,n,k}(\zeta_{m,n};f_n^{s-1}) \in \{1,-1\} \\ |\zeta_{m,n} - f_m^{s-1}| < \frac{1}{2|\tau_{m,k}|} \end{cases} \tag{13}$$

and thus solve $\{\kappa_{m,n,k}, \zeta_{m,n,k}, \delta_{m,n,k}\}$ based on (13) and the sign of $y_{m,n,k}'(f_m;f_n^{s-1})$ at f_m^{s-1}, i.e,

$$\tilde{y}_{m,n,k}'(f_m^{s-1};f_n^{s-1}) = -2\pi\tau_{m,k}\sin[2\pi(f_m^{s-1}\tau_{m,k} - f_n^{s-1}\tau_{n,k})].$$

More specifically, if $y_{m,n,k}'(f_m^{s-1};f_n^{s-1}) = 0$, we have

$$\begin{cases} \kappa_{m,n,k} = -(1+\delta_{m,n,k})\pi^2\tau_{m,k}^2, \\ \zeta_{m,n,k} = f_m^{s-1}, \\ \delta_{m,n,k} = \cos[2\pi(f_m^{s-1}\tau_{m,k} - f_n^{s-1}\tau_{n,k})] \in \{1,-1\} \end{cases} \tag{14}$$

Otherwise, we have

$$\begin{cases} \kappa_{m,n,k} = \dfrac{-\pi\tau_{m,k}\sin[2\pi(f_m^{s-1}\tau_{m,k} - f_n^{s-1}\tau_{n,k})]}{f_m^{s-1} - \zeta_{m,n,k}} \\ \zeta_{m,n,k} = \begin{cases} \dfrac{\lceil(f_m^{s-1}\tau_{m,k} - f_n^{s-1}\tau_{n,k})\rceil + f_n^{s-1}\tau_{n,k}}{\tau_{m,k}}, \\ \hfill \text{if } y_{m,n,k}'(f_m^{s-1};f_n^{s-1}) > 0 \\ \dfrac{\lfloor(f_m^{s-1}\tau_{m,k} - f_n^{s-1}\tau_{n,k})\rfloor + f_n^{s-1}\tau_{n,k}}{\tau_{m,k}}, \\ \hfill \text{if } y_{m,n,k}'(f_m^{s-1};f_n^{s-1}) < 0 \end{cases} \\ \delta_{m,n,k} = \cos[2\pi(f_m^{s-1}\tau_{m,k} - f_n^{s-1}\tau_{n,k})] \\ \hfill - \kappa_{m,n,k}(f_m^{s-1} - \zeta_{m,n,k})^2, \end{cases} \tag{15}$$

where $\lfloor\cdot\rfloor$ and $\lceil\cdot\rceil$ round the argument to the nearest integer towards $-\infty$ and ∞, respectively.

4. NUMERICAL SIMULATIONS

We consider a transmit array operating at $f_c = 60$GHz, and the upper bound of frequency offsets is set as $\Delta F = 10^{-5} f_c = 600$kHz.

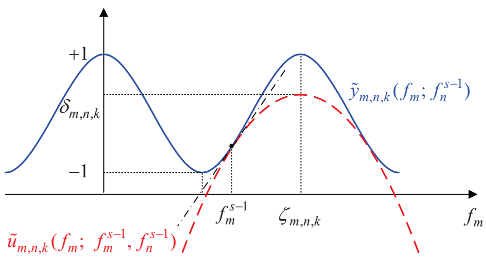

Fig. 2. Approximate the $\cos(\cdot)$ by a concave quadratic function.

Table 1: Algorithm 1 for frequency offsets design

Find a feasible point $\mathbf{f}^0$ and set $s = 0$;
repeat
  $s = s + 1,\ m = (s \bmod M) + 1;$
  Design $\{\kappa_{m,n,k}, \zeta_{m,n,k}, \delta_{m,n,k}\}$ by (14) and (15);
  $f_m^s = \left[\frac{\sum_{k=1}^{K} a^2(r_k)\sum_{n=1}^{M}\kappa_{m,n,k}\zeta_{m,n,k}}{\sum_{k=1}^{K} a^2(r_k)\sum_{n=1}^{M}\kappa_{m,n,k}}\right]_{f_c-\Delta F}^{f_c+\Delta F};$
  $f_n^s = f_n^{s-1},\ \ \forall\, n \neq m;$
until some stopping criterion is satisfied.

To focus on the FDA beampattern characteristics, we ignore the signal attenuation factor and fix $a(r) = 1$. We consider two typical user traces, i.e., linear trace and spiral trace. In the linear trace setting, the user starts from the point $(r = 500\text{m}, \theta = 0^{\text{o}})$ and moves in parallel with the array, at a speed of 100m/s or 360km/h. In the spiral trace setting, the user starts from the point $(r = 100\text{m}, \theta = -30^{\text{o}})$ and moves at the range speed of 100m/s plus the angle speed of $10^{\text{o}}/\text{s}$. In the following simulations, we define the time period as $[T_1 = 1\text{s}, T_2 = 10\text{s}]$, and compare the average beampattern gains of the PDA approach utilizing only one group of phase shifters and the FDA approach utilizing only one group of frequency offsets.

Fig. 3 shows the converging behaviour of the BSUM algorithm (cf. Table 1), with each trace starting from a randomly selected initial point. Typically, for $M = 8$ antennas arrays, the BSUM algorithm converges in about 60 iterations.

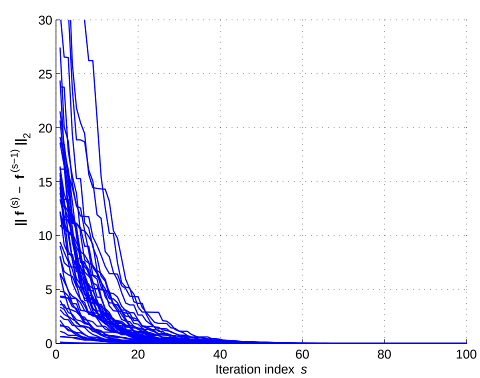

Fig. 3. Typical converging traces of the BSUM algorithm.

Next, we compare the average beampattern gains of the PDA and FDA approaches for different antenna numbers. The results are displayed in Fig. 4. In general, the beampattern gain increases with M since more spatial diversity can be achieved. For the tested two user traces, the FDA approach outperforms the conventional PDA approach clearly. This is expected since in the proposed approach, we optimize the frequency offsets such that the beampattern peak trace fits the user trace maximally.

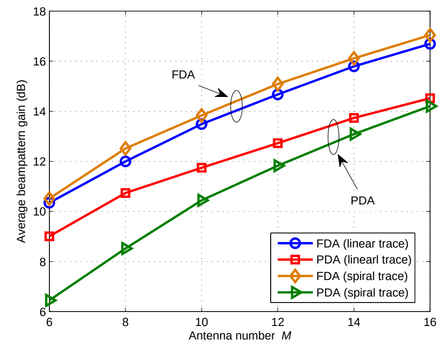

Fig. 4. Average beampattern gain comparison for different M.

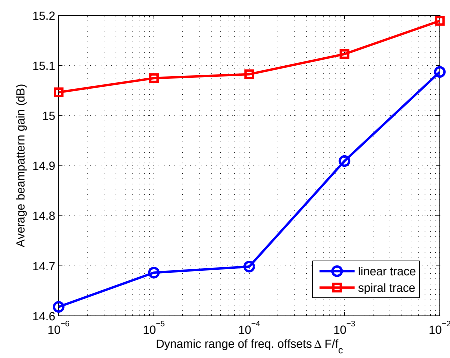

Fig. 5. Average beampattern gain comparison for different ΔF.

We should mention that the FDA approach improves the average beampattern gain at the expense of wider frequency band. Actually, introducing the frequency offsets renders some transmit bandwidth expansion. On the other hand, ΔF is required to be far less than the carrier frequency f_c in practice [18]. Therefore, we should balance the performance improvement and the bandwidth expansion. In Fig. 5, we show how ΔF influences the FDA performance for $M = 12$. As expected, increasing ΔF provides more flexibilities in frequency offsets design, and thus improves the average beampattern gain. As the expense, wider transmit band is needed.

5. CONCLUSIONS

We propose a novel FDA approach to achieve accompanying beampattern peak for high-speed users. It differs from the PDA approach by employing some frequency offsets across the array such that an angle-range-time dependent beampattern is generated. In this paper, we optimize the frequency offsets to maximize the average beampattern gain along the user trace. A BSUM-based algorithm is developed to find a stationary solution. Compared with PDA approaches, the FDA approach maintains high service quality for quickly-moving users by updating frequency offsets less frequently, thus reducing the implementation cost considerably. Its efficacy has been demonstrated by numerical simulations.

6. REFERENCES

[1] Xinhua News Agency, “China’s new high-speed train debuts on Beijing-Shanghai route,” Jun. 26, 2017. Available online at: http://en.people.cn/n3/2017/0626/c90000-9233299.html

[2] L.C. Godara, *Smart Antennas*, CRC Press LLC, 2004.

[3] B. Allen and M. Ghavami, *Adapative Array Systems: Fundamentals and Applications*, Wiley, New York, 2006.

[4] P. Antonik, M.C. Wicks, H.D. Griffiths, and C.J. Baker, “Frequency diverse array radars,” in *Proc. IEEE Radar Conf.*, pp. 215-217, Verona, April 2006.

[5] P. Antonik, “An investigation of a frequency diverse array,” PhD dissertation, University College London, 2009.

[6] W.-Q. Wang, “Overview of frequency diverse array in radar and navigation applications,” *IET Radar, Sonar & Navigation*, vol. 10, no. 6, pp. 1001–1012, Jun. 2016.

[7] S. Mustafa, D. Simsek, and H.A.E. Taylan, “Frequency diverse array antenna with periodic time modulated pattern in range and angle,” in *Proc. IEEE Radar Conf.*, pp. 427–430, Boston, April 2007.

[8] W.-Q. Wang, and H.C. So, “Transmit subaperturing for range and angle estimation in frequency diverse array radar,” *IEEE Trans. Signal Processing*, vol. 62, no. 8, pp. 2000-2011, April 2014.

[9] S. Huang, K.F. Tong and C.J. Baker “Frequency diverse array with beam scanning feature,” in *Proc. IEEE Antennas and Propagation Conf.*, pp. 1–4, San Diego, California, July 2008.

[10] P.F. Sammartino, C.J. Baker, and H.D. Griffiths, “Frequency diverse MIMO techniques for radar,” *IEEE Trans. Aerosp. Electron. Syst.*, vol. 49, no. 1, pp. 201–222, Jan. 2013.

[11] Y. Ding, J. Zhang and V. Fusco, “Frequency diverse array OFDM transmitter for secure wireless communication,” *Electronic Letters*, vol. 51, no. 17, pp. 1374–1376, Aug. 2015.

[12] J. Hu, S. Yan, F. Shu, J. Wang and Y. Zhang, “Artificial-noise-aided secure transmission with directional modulation based on random frequency diverse arrays,” *IEEE Access*, vol. 5, pp. 1658-1667, Jan. 2017.

[13] J. Xiong, S.Y. Nusenu and W.-Q. Wang, “Directional modulation using frequency diverse array for secure communications,” *Wireless Personal Communications* , vol. 95, no. 3, pp. 2679–2689, 2017.

[14] J. Lin, Q. Li, J. Yang, H. Shao, and W.-Q. Wang, “Physical-layer security for proximal legitimate user and evavesdropper: a frequency diverse array beamforming approach,” *IEEE Trans. Information Forensics and Security*, vol. 13, no. 3, pp. 671–684, Mar. 2018.

[15] M. Razaviyayn, M. Hong, and Z.-Q. Luo, “A unified convergence analysis of block successive minimization methods for nonsmooth optimization,” *SIAM Journal on Optimization*, vol. 23, no. 2, pp. 1126–1153, June 2013.

[16] MiWEBA, “Millimetre-wave evolution for backhaul and access,” *MiWEBA Technical Reports*, June 2014.

[17] P. Tseng, “Convergene of a block coordinate descent method for nondifferentiable minimization,” *Journal of Optimization Theory and Applications*, vol. 109, no. 3, pp. 475–494, June 2001.

[18] C. Cetinepe and S. Demir, “Multipath characteristics of frequency diverse arrays over a ground plane,” *IEEE Trans. Antennas and Propagation*, vol. 62, no. 7, pp. 3567–3574, July 2014.